

# Temporal fine structure of nighttime spike events in auroral radio absorption, studied by a wavelet method

J.K. Hargreaves<sup>1</sup>

Department of Communication Systems, University of Lancaster, Bailrigg, Lancaster England

A. Ranta

Sodankylä Geophysical Observatory, Sodankylä, Finland

J. D. Annan, J. C. Hargreaves

Proudman Oceanographic Laboratory, Bidston Observatory, Prenton, Merseyside, England

**Abstract.** The auroral absorption spike event, occurring generally at the onset of a substorm, is distinguished by its high intensity and short duration. This paper reports the presence of a fine structure within the spike event. Analysis of selected examples using the Morlet wavelet shows that within the 1–2 min duration of the spike are significant modulations with periodicities in the bands 15–60 s (67–16 mHz), and 5–10 s (200–100 mHz), the former being the stronger. The slower fluctuations can amount to more than 10% of the absorption, and they were observed in every example (seven out of nine) in which the spike was moving poleward. They were absent in the other two cases, when the spike moved equatorward. In the examples studied, the 15–60 s absorption pulsations were accompanied by magnetic micropulsations of impulsive type (*Pi*) having a periodicity that was similar or harmonically related. The connection is only close while the spike event is moving. Consideration of the details suggests that both the magnetic and the absorption pulsations are related to the acceleration process at substorm onset, the flux of energetic particles into the auroral zone producing the radio absorption being modulated with, though not by, the geomagnetic field variations. The 5–10 s pulsations, which are considerably weaker, appeared in both the absorption and the magnetic records, but in this case with no obvious connection between them.

## 1. Introduction

In auroral radio absorption, as observed with riometer, the spike event is one of the more intensively studied features. Its relatively large magnitude and short duration make it easily recognized, and with the application of imaging riometry [Detrick and Rosenberg, 1990] the essential spatial and dynamic characteristics have been identified [Hargreaves et al., 1997]. Thus the generally poleward motion of the event, at least for those occurring at the beginning of a substorm, has been confirmed for activity at Kilpisjärvi and South Pole. The spatial extent (167 km by 74 km was the median result) has been measured, and the duration of the event has been determined as 1–2 min. These facts can be stated with some confidence because many spike events develop, move, and decay within the field of view of a single imaging riometer system.

The imaging riometer at Kilpisjärvi (69.05°N, 20.79°E, L = 5.9) records at a 1 s interval, but the data are usually averaged over 10 s or 1 min to improve the accuracy of measurement. However, the 1 s data are usable for the more intense events, and this includes many of the spikes, a significant number of which amount to several decibels and may be as strong as 12 or 14 dB. Using these data, Ranta et al. [1999] observed fine structure within two spike events showing periodicities in the range 2–9 s and 30–90 s.

The study has now been extended to a larger selection of events, and a more objective method has been used to identify and describe the fine structure.

## 2. Wavelet Analysis

Auroral radio absorption is nonstationary in the statistical sense. It occurs in "events" of limited duration, and the spectral structure represented by the series of absorption against time changes during the event. The results of a standard spectral analysis, for example by Fourier analysis, therefore depend on the time interval

Copyright 2001 by the American Geophysical Union.

Paper number 2001JA900008.

0148-0227/01/2001JA900008\$09.00

selected. The periodicities that occur, moreover, may well appear for a few cycles only, and further judgment is required as to how to handle this feature. There is therefore a subjective element in the results.

In a wavelet analysis [Torrence and Compo, 1998], the time series is convolved with "wavelets" of limited duration, and this procedure is able to bring out, within limits of temporal and spatial resolution, the evolution of the spectrum through the event.

The form of the wavelet has to be decided, but then the results are objective. The wavelet used here has the Morlet form [Morlet et al. 1982]

$$\frac{1}{a^{\frac{1}{2}}} e^{\frac{jk(t-b)}{a}} e^{[-\frac{(t-b)}{a}]^2}, \quad (1)$$

where  $t$  is time and  $k$  is a constant here equal to 5.4. Here  $k$  determines how many oscillations of the second term are contained within the envelope set by the third term. The parameter  $a$  is varied to alter the periodicity selected, which is given by  $P = 1.16a$  (when  $k = 5.4$ ). The real part of equation (1) is a maximum at  $t = 0$ , and the next positive maximum, when  $\frac{t}{a} = \pm 1.16$ , is smaller by a factor 0.51. The next maximum is only 0.07 of the central maximum. Thus the time resolution is about two periods. In the present work,  $a$  is stepped by a factor of  $2^{0.2}$  ( $= 1.149$ ) over 41 values covering the 2 to 512 s period (and 500 to 1.95 mHz in frequency), and  $b$  is the translation of the wavelet in time. The frequency resolution is about 32% of the center frequency.

### 3. Data

Nine examples of intense but short-duration absorption events were selected for analysis (Table 1). Micropulsation data, also from Kilpisjärvi, were available for five of the events. For the other four events the magnetic data were either not available or not of adequate quality. Figure 1 shows the signatures of the absorption events as recorded by the wide-beam, 38.2 MHz riometer at Kilpisjärvi. Most of these events showed the characteristics of a classical spike at substorm onset, having a sharp onset and being closely followed by a main substorm phase. Examination of the imaging riometer data showed that most of them also had a well-defined poleward motion. (As pointed out by Hargreaves et al. [1997], all spikes of this kind seem to have a poleward component of motion, whereas the E-W component of motion can be either east-to-west or west-to-east.)

Events 1 and 2 were more isolated in the sense that they were not followed immediately (i.e., within about 5 min) by main phase absorption of longer duration, though there was further activity after 20–30 min. The westward motion was dominant in each of these cases, and event 1 crossed the whole field of view from east to west. This event was probably a westward traveling surge (WTS) (of which more later), and event 2 might also have been such.

Event 7 has a somewhat different appearance, being isolated but with not such a sharp onset. This event showed equatorward motion, as did event 8. We therefore suppose that these two events may have been of a different kind from the others.

These plots, which are at 10 s resolution, do not show enough fine structure on the scale of a minute or less to arouse interest. However, when the 1 s data are inspected, a well-defined fine structure is seen, as illustrated in the lower plots of Figures 2 and 3. The absorption plotted here is not that observed in any single beam of the system, but is the greatest value over the whole array irrespective of location. This technique separates changes within the event from the effects of event movement (which may also be plotted from the changing position of the maximum).

When viewed thus, the spike event is observed to be larger than the wide-beam indication by a factor between 1.7 and 3.0. This ratio is typical of nighttime spike events [Hargreaves et al. 1997] and is due to the relatively small spatial scale of this type of event. Of the set of nine selected for study, only event 7 showed no fine structure.

### 4. Wavelet Spectra

On analysis using the Morlet wavelet (equation (1)), most of the events show a characteristic spectrum, of which the upper diagrams of Figures 2 and 3 are typical. Both those examples show spectral maxima at 41 mHz (24 s period). In each event of the set (Table 2), at least one maximum appears between 18 and 62 mHz (periods 56 to 16 s) and the bandwidth of this feature is in the range 15 to 26 mHz. (The bandwidth is defined as the difference between the frequencies where the power density is half that at the peak.) The contours in Figures 2 and 3 are linear in power spectral density. If the plot is made over a range of smaller values instead, a range of weaker features comes into view, having frequencies 109 to 165 mHz, equivalent to periodicities between 9.2 and 6.1 s (Table 2). Using a logarithmic scale of power density as in Figure 4, the periodicities in both ranges may be seen together and their incidence compared with the original record of absorption against time. In this example (event 5) the shorter periodicity occurred in the leading edge of the event and again just following its maximum, but as may be noted from the table, there appears to be no rule about this. While the longer periodicity always appears during the peak of the event, the shorter one can be in the rising edge, near the peak or in the decline.

Event 5 continued for about 5 min instead of the more usual 2 min, and a poleward/westward movement occurred twice. However, the spectral signature noted above was observed only once, during the first part of the event. Evidently, the structure in the later part lacked the coherence for it to be recognized by the

Table 1. Spike Events Selected for Analysis

Event	Date	Day of Year	UT	Number of Is Points	Maximum Absorption (dB)	Motion of Absorption peak	Comments	Fine Structure ?	Maximum Amplitude of Magnetic Pulsation (nT)	Maximum Absorption/Wide-Beam Absorption
1	Dec.11,1994	345	1743-1748	360	12.6	E→W Some S→N	isolated; may be W T S	Yes	-	3.0
2	Jan.5, 1995	005	1817-1822	360	13.2	E→W S→N	isolated	Yes	-	2.3
3	Jan.30,1995	030	1736-1740	300	9.1	E→W S→N	classic spike at event onset	Yes	-	2.0
4	Feb.13,1995	044	2050-2055	360	12.3	E→W S→N	classic spike at event onset	Yes	-	2.9
5	Oct.6,1994	279	2046-2051	360	8.2	W→E S→N	motion repeated	Yes	1160	2.7
6	Jan.28,1997	028	2030-2100	1800	7.9	E→W S→N	sharp onset, structured event	Yes	1790	3.0
7	Feb.9,1997	040	2000-2010	600	12.3	W→E N→S	isolated but symmetrical	No	420	1.7
8	March 28,1997	087	2010-2030	1200	5.2	W→E N→S	sharp onset	Yes	1160	1.9
9	March 29,1997	088	2215-2225	600	7.6	E→W S→N	classic spike at event onset	Yes	700	2.8

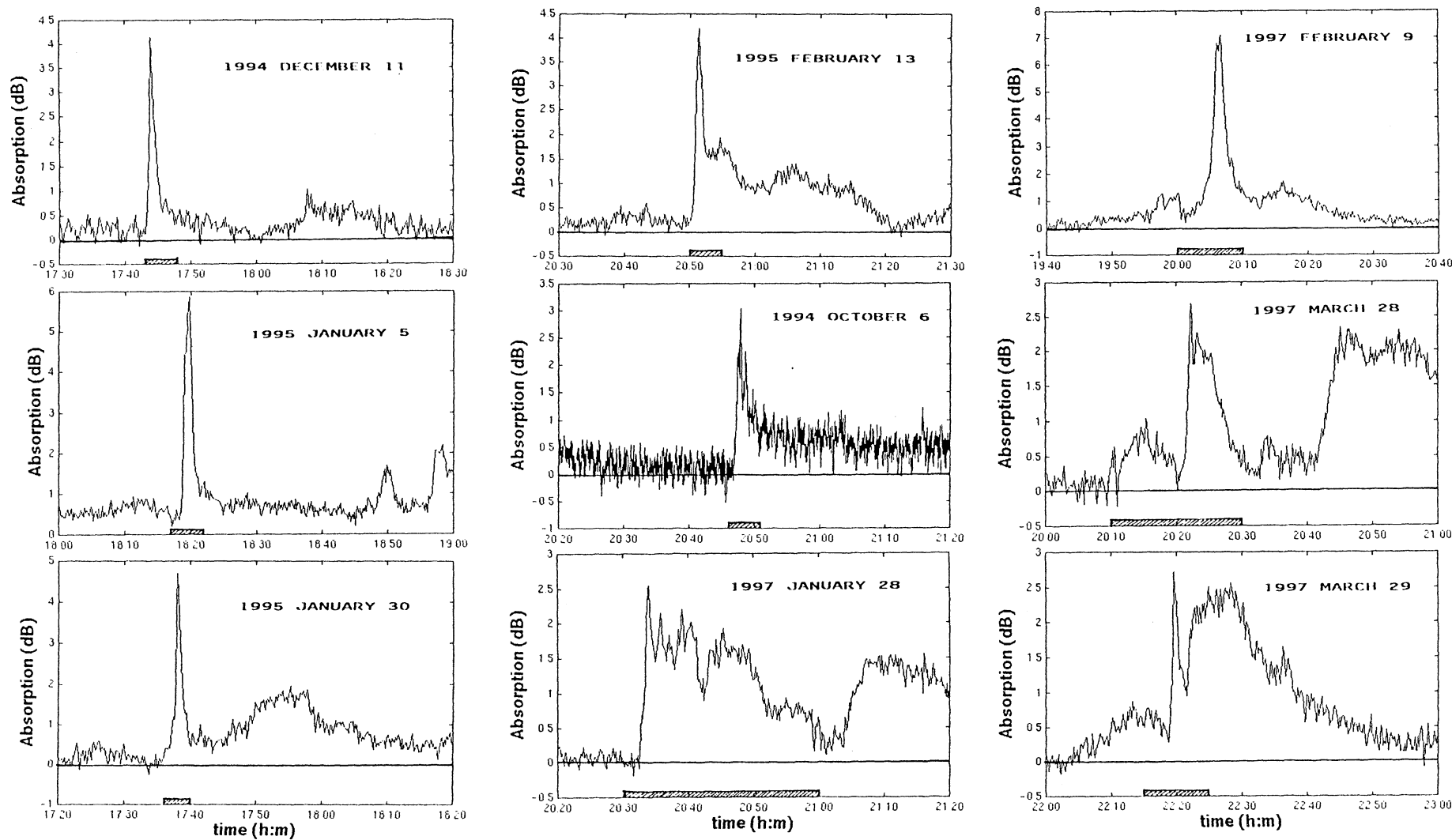
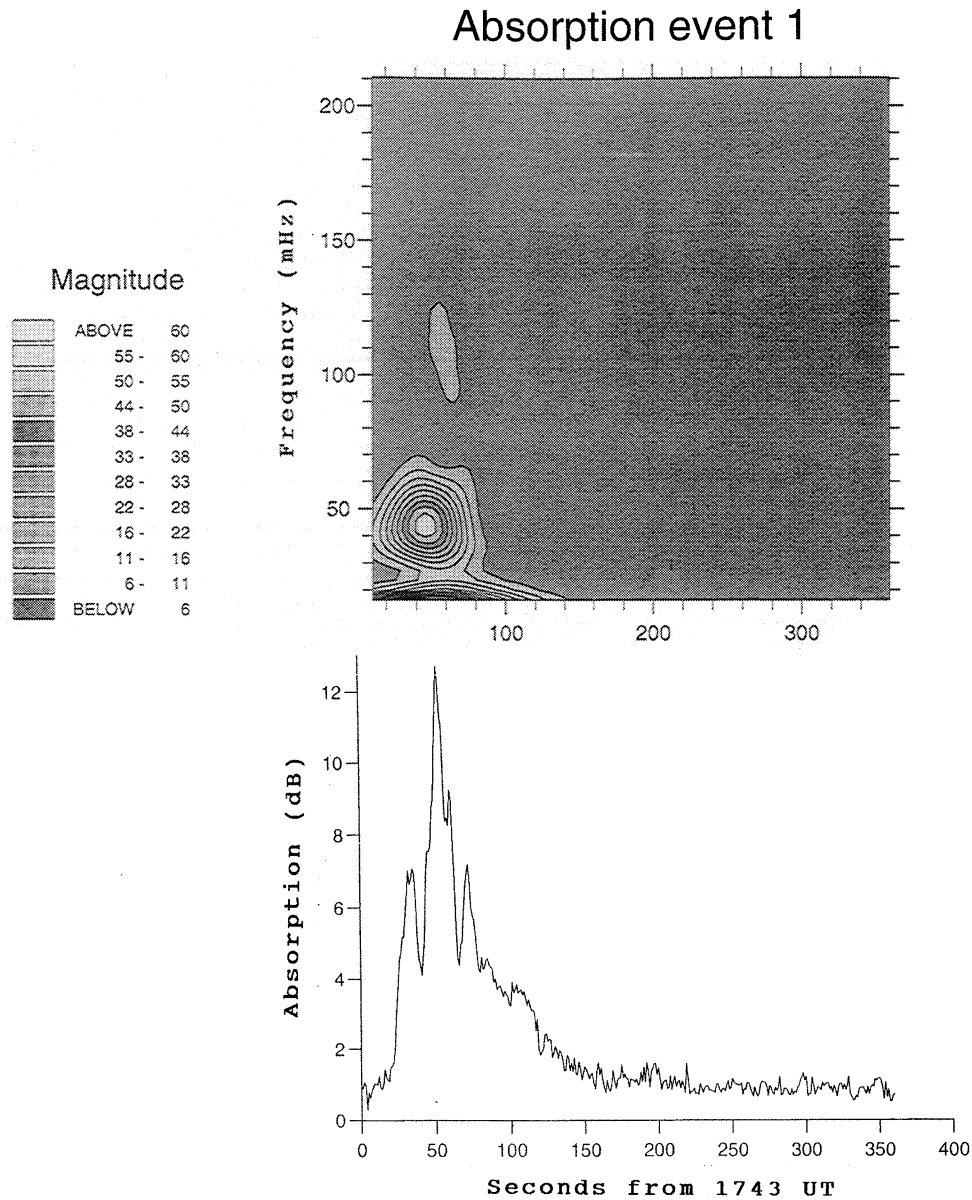


Figure 1. The nine spike events selected for the study, as registered by the 38.2 MHz widebeam riometer at Kilpisjärvi. At 10 s resolution there is little or no indication of fine structure.



**Figure 2.** Wavelet spectrum and absorption against time for event 1 (December 11, 1994, 1743 - 1748 UT). The absorption plotted here and in other examples is the greatest value observed over the whole imaging riometer array.

wavelets. This seems to be a common pattern in longer events, the periodicity being restricted to the first burst of activity. Moreover, event 8, though showing time structure when plotted at 1 s resolution, also fails to show a coherent periodicity. The spectrum is a continuum, intensity decreasing with increasing frequency and without discrete maxima. This, like the smoother event 7, is characterized by equatorward rather than poleward motion. On the evidence of the present selection, therefore, we conclude that periodicities are confined to spikes having poleward motion only, and are most likely to occur within 2 min of the start of the event. On the other hand, both longer (16 - 56 s) and shorter (6.1 - 9.2 s) periodicities (frequencies 62 - 18 mHz and 164 - 109 mHz, respectively) occurred in each

of the seven examples (events 1, 2, 3, 4, 5, 6, and 9) where the spike moved poleward.

In two cases (5 and 6), two periodicities in the range 15 to 56 s (or 67 - 18 mHz) were noted, one being the second harmonic of the other.

These spectra are unlikely to have arisen by chance. An analysis of random noise using the same Morlet wavelet (Figure 5) produced an irregular spectrum in which the spectral maxima are distributed randomly over the frequency-time plot. The overall appearance is markedly different from those derived from the absorption events, though individual maxima are similar in duration and bandwidth, this no doubt representing the properties of the wavelet. Considering the foregoing point, the element of consistency between the spectra

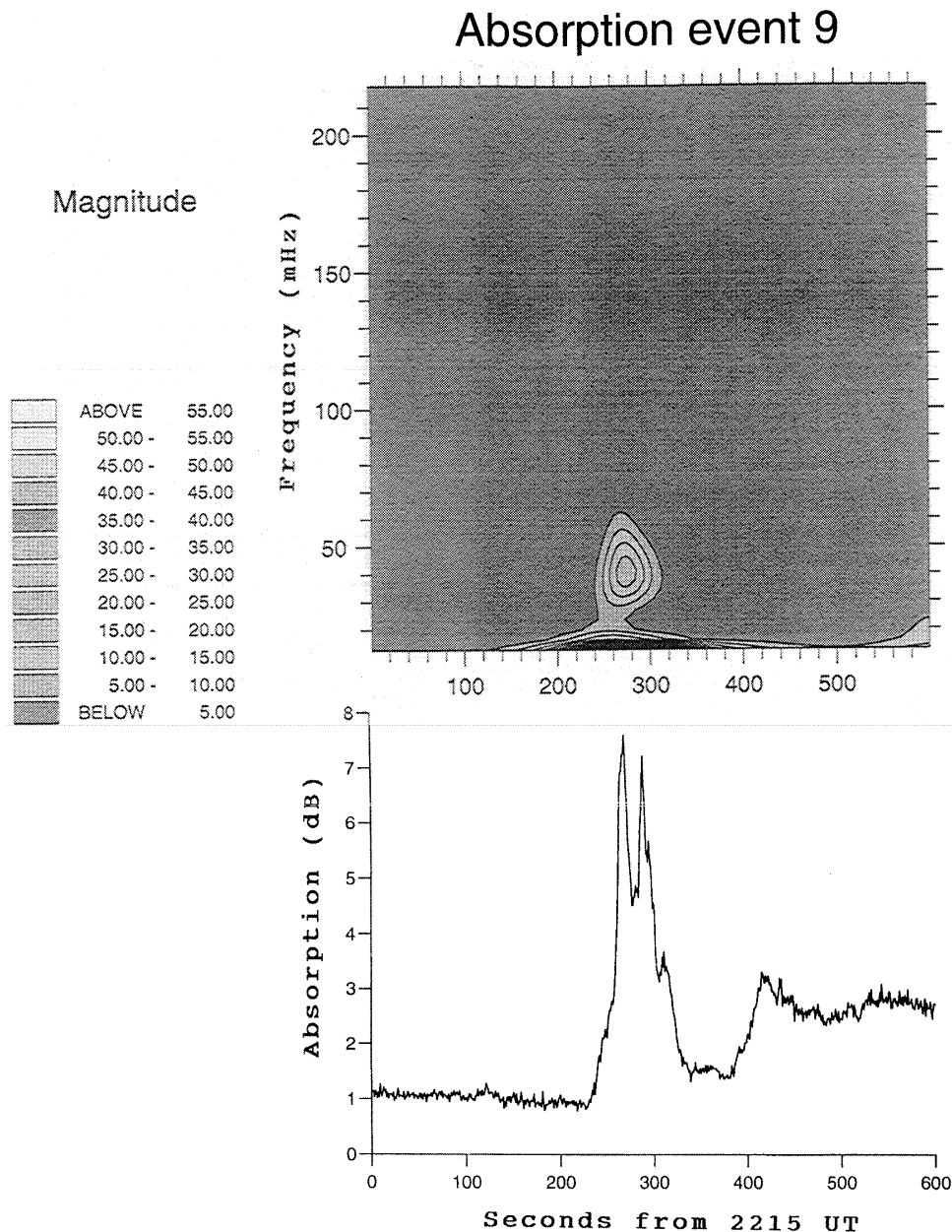


**Figure 3.** Wavelet spectrum and absorption against time for event 9 (March 29, 1997, 2215 - 2225 UT).

of different spike events, and the consistency between the periodicities indicated by the spectra and the fluctuations visible in the 1 s absorption plots, it seems reasonable to accept the quasi-periodic modulation of spike events as an observed fact.

## 5. Filtering by Means of Wavelets

Filtering may be achieved by taking a band of wavelets and performing an inversion; this provides a visual impression of the signal in that band in both amplitude and phase. The bands were selected to isolate the main periodicities noted on the wavelet spectra. In Figure 6, event 3 has been filtered in three bands: 0–16

mHz (filter 1a), 16–35 mHz (filter 1b), and 116–180 mHz (filter 2). In the time domain these correspond to infinity to 62.5 s, 62.5 to 28.6 s, and 8.6 to 5.6 s, respectively. The unfiltered absorption is shown for comparison (but displaced for clarity). Filter 1b isolates the 42 s periodicity (24 mHz), having amplitude up to 1.2 dB. Filter 2 shows the 6.5 s periodicity (154 mHz), whose amplitude does not exceed 0.6 dB. (Compare these values with the rms amplitudes in Table 2.) We note that the 42 s component appears for about two cycles, and its effect is clearly seen in the original record. The shorter one (6.5 s) is present, though somewhat less strongly, for about five cycles, and it occurs again at a low level at other times during the event. This component may

Table 2. Spectral Features in Absorption Events

Event	Maximum Point	UT	Frequency mHz	Period s	Power Density (dB) <sup>2</sup> /Hz	Bandwidth mHz	Max Power (dB) <sup>2</sup>	Equivalent rms Amplitude dB	Remarks
1	59	1732:58	109	9.2	9.6	58	0.56	0.75	declining edge of event
	47	1743:48	41	24	57	24	1.37	1.17	
2	160	1819:39	125	8.0	2.1	71	0.15	0.39	declining edge of event
	129	1819:09	54	18	22	24	0.53	0.73	
3	101	1737:40	154	6.5	2.8	64	0.18	0.42	at peak of event
	112	1737:51	24	42	25	~18	0.45	0.67	
4	55	2050:54	144	6.9	0.71	55	0.039	0.20	just before peak of event
	81	2051:20	24	42	26	~18	0.47	0.68	
5	74	2047:13	109	9.2	3.8	51	0.19	0.44	Leading edge of event follows main event points 105 and 101 are almost coincident
	186	2049:05	109	9.2	1.2	54	0.065	0.25	
	105	2047:44	62.5	16	6.8	26	0.18	0.42	
	101	2047:40	31	32	54	15	0.81	0.90	
6	162	2032:41	165	6.1	0.80	45	0.036	0.19	just before peak of event
	227	2033:46	36	28	30	22	0.66	0.81	
	194	2033:13	18	56	48	16	0.77	0.88	
9	289	2219:48	109	9.2	1.4	52	0.073	0.27	just before peak of event
	274	2219:33	41	24	25	22	0.55	0.74	

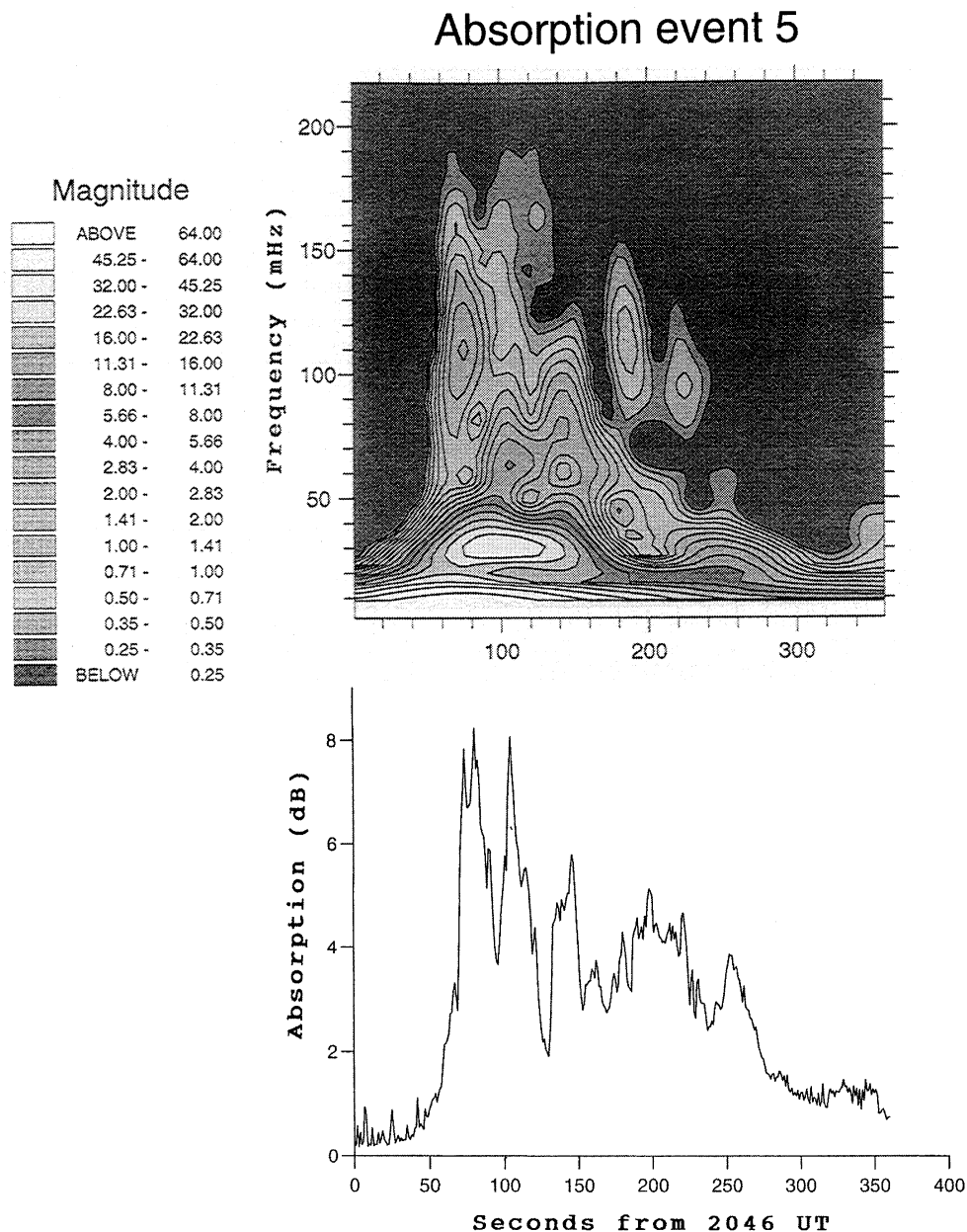


**Figure 4.** Wavelet spectrum and absorption against time for event 5 (October 6, 1994, 2046 - 2051 UT). The power density is here plotted on a logarithmic scale, to show both the lower (31 mHz) and the higher (9.2 s) frequencies. Note the harmonic at time 105 s and frequency 62 mHz.

also be seen in the original record, though its properties could not have been estimated with any accuracy without the analysis.

## 6. Relation to Magnetic Micropulsations

Irregular pulsations of period 1 – 40 s (Pi1) and 40 – 150 s or greater (Pi2) are well known in the records from magnetometers and other ground-based magnetic detectors [Jacobs, 1970]. They are also seen on satellite-borne magnetometers [McPherron, 1981]. It is clear, therefore, that they exist in the magnetosphere and are not merely ionospheric phenomena. Of particu-

lar importance was the discovery that Pi2 occurrence is associated with the beginning of substorms [Coroniti *et al.*, 1968]; indeed, Pi2 is often considered one of the definitive signatures of substorm commencement, though questions have been raised about the precise timing [Liou *et al.*, 2000]. In particular, a burst of Pi2 seems to coincide with the westward traveling surge (WTS) in the luminous aurora [Pashin *et al.*, 1982; Samson and Rostoker, 1983], the feature that generally precedes auroral breakup.

Magnetic data were therefore obtained for some of the absorption events studied here, in order (1) to see whether Pi2 occurs at the same time as the spike event, (2) to look for any similarity of periodicity or of coher-



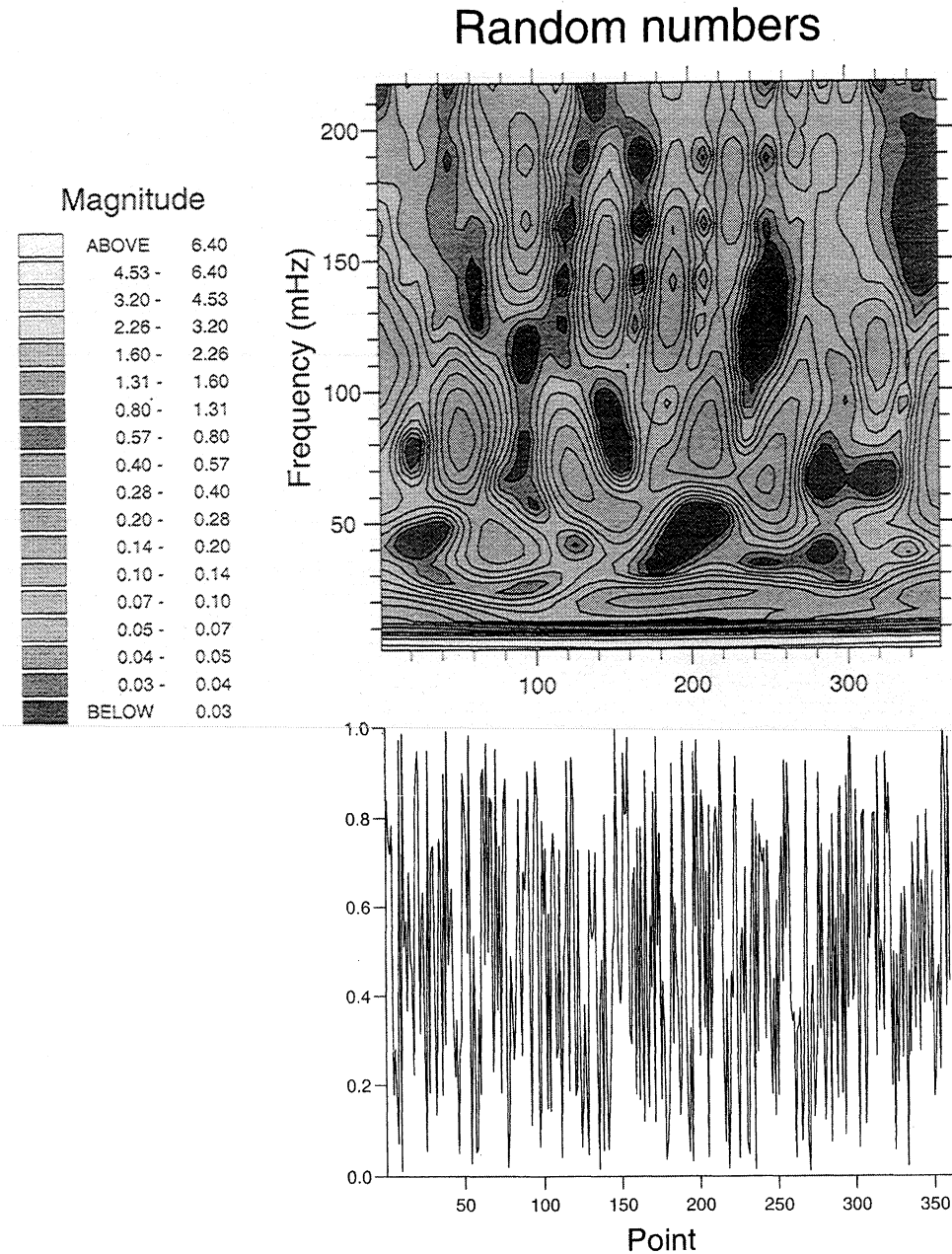


Figure 5. Analysis of random noise.

ence between the waveforms in the two phenomena, and (3) to seek any evidence of a causal relationship.

Figure 7 shows the magnetic record from Kilpisjärvi during absorption event 5, and its wavelet analysis carried out in exactly the same way. The signal is seen to vary with time in an almost regular manner, and there is a clear maximum in the spectrum at 29 mHz (period 34 s). This occurs at the same time as the same periodicity (31 mHz) appears in the absorption spectrum shown in Figure 4. It also reappears 140 s later, when there is no maximum in the absorption spectrum. The filtered bands 24 – 38.5 mHz (42 – 26 s) for the magnetic signal and the absorption are compared in Figure 8a, and there is a remarkable phase coherence between them.

At time 240 s the magnetic fluctuation is strong and the absorption fluctuation has become much weaker, but the phase relation is maintained. In the example of event 5, therefore, the principal fluctuations in the absorption and in the magnetic field are at virtually the same frequency and are in phase throughout. However, the absorption fluctuation is much stronger near the start of the event than later, while the magnetic Pi is as strong or stronger toward the end of the event.

The same sort of correspondence is not found with regard to the 9.2 s periodicity (109 mHz) that occurs near the point 74 s from the beginning of absorption event 5. The magnetic record shows no maximum at or near this period between times 50 s and 100 s, and

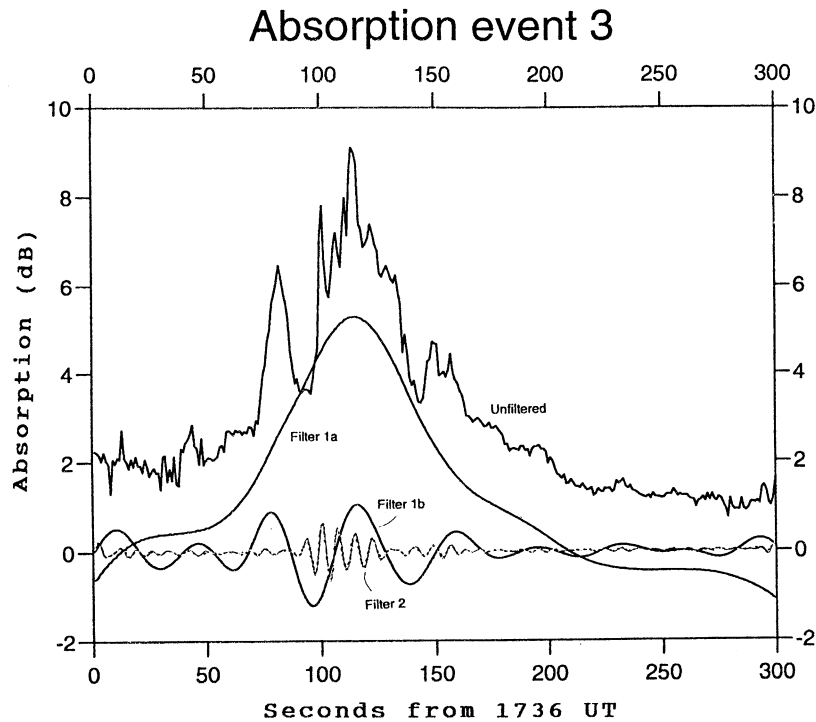


**Figure 6.** Filtering of event 3 (January 30, 1995, 1736 - 1740 UT), by Morlet wavelets. Filter 1a (below 16 mHz) shows the smoothed form of the spike, filter 1b (16 - 35 mHz) selects the periodicity at 42 s (24 mHz), and filter 2 (116 - 180 mHz) isolates the weak periodicity at 6.5 s (154 mHz).

if the two sets of data filtered for the band 84 - 115 mHz (11.0 - 8.7 s) are compared in details no consistent phase relationship is seen (Figure 8b).

Since the typical absorption spike lasts no more than 2 - 3 min, a sample of 5 - 6 min should be ample for studying the structure of the event. Some data, however, were taken over a longer period in order to see whether there is any connection between the respective bursts of magnetic and absorption activity seen as a whole. Event 6 was taken over 30 min. The pulsation begins sharply about the same time as the onset of absorption, and is strongest during the early part of the event before about 300 s, the interval when the absorption is also most intense. However, it is also strong around 900 s when the absorption has declined, and it continues at a significant level as the absorption fades toward the end of the period. (See Figure 9.) The pulsations may be seen in more detail in the expanded plot of Figure 10. This also shows that only the early part of the absorption event has the poleward motion typical of the spike event. The later part, after 300 s, may look the same on an absorption-time plot, but the dynamics are different, the absorption patch being considerably more static.

The results indicate that the intensities of absorption and magnetic pulsation are related when the activity begins (i.e., during the poleward - moving spike event) but not subsequently. The two phenomena tend to begin together, but the magnetic pulsation tends to

continue for longer. The behavior in event 5, discussed above, is consistent with this. Event 9 tells much the same story, having a well-defined magnetic pulsation not only during the spike event, but also continuing for at least 300 s after the spike event has ended. It is conceivable that the source of magnetic pulsation has moved outside the viewing area of the riometer in these cases.

Table 3 summarizes the periodicities in the micropulsations revealed by the wavelet analyses. As stated above, the coincidence of absorption and magnetic pulsations near 30 s period in event 5 is remarkably similar in time, frequency, and phase. In event 6 (Figure 11) the main features near times 230 - 240 s differ somewhat in frequency between the absorption (36 mHz) and the magnetic (46 mHz) records but overlap considerably if the bandwidth (22 and 32 mHz) is taken into account. The absorption spectrum also has a peak at 18 mHz (56 s), and the magnetic record shows some enhancement at about the same frequency some 40 s (one cycle) later. The case of event 9 is more complicated. The magnetic and absorption activity obviously begin about the same time (within 20 s), but the main absorption feature at 41 mHz (24 s), occurring 274 s into the event, lies midway between peaks at 20 and 61 mHz (50 and 17 s) in the magnetic spectrum (Figure 12). There appear to be harmonic relationships here.

No clear associations of this kind have been seen between the fluctuations of shorter period, though their

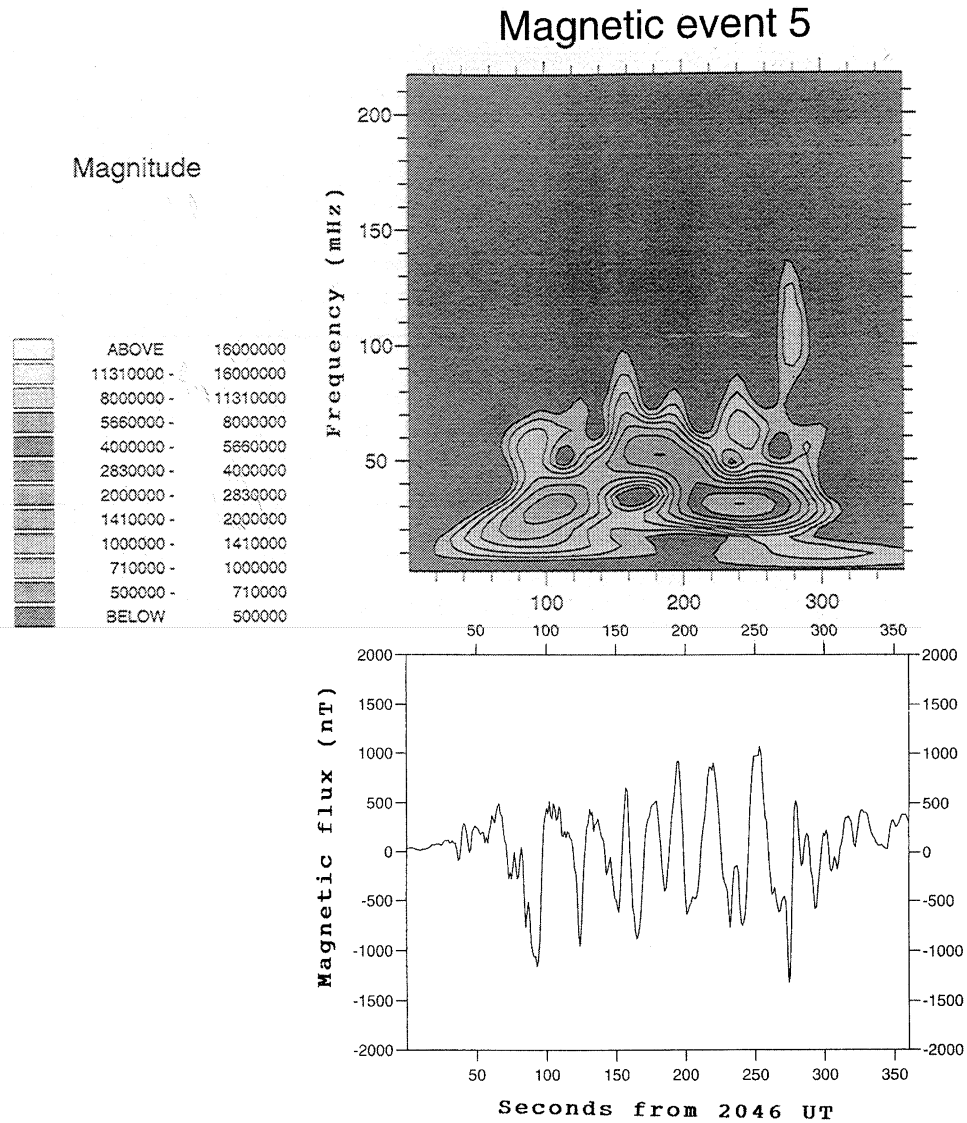
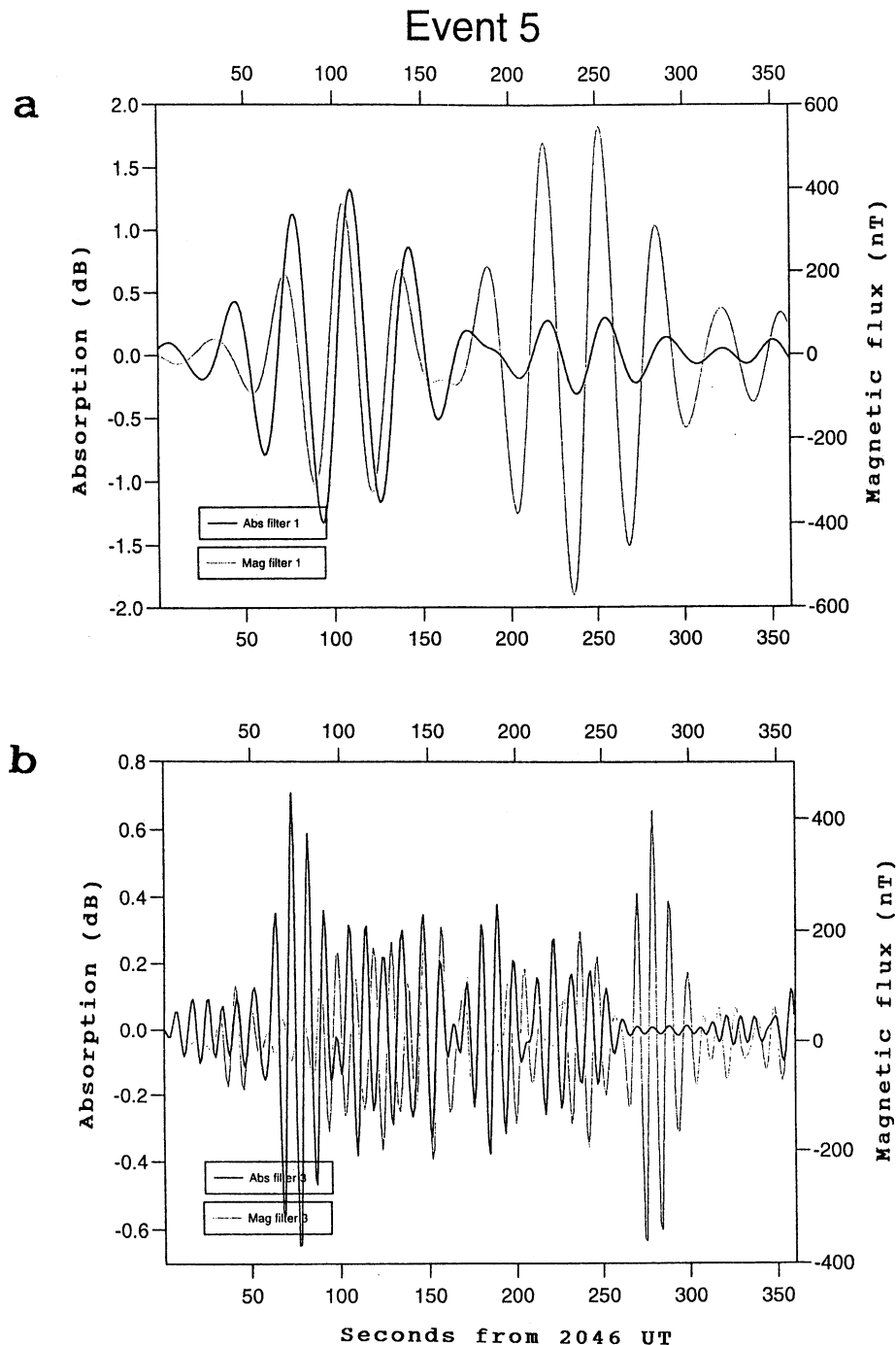


Figure 7. Wavelet spectrum and magnetic record for event 5. Compare this with Figure 4.

Table 3. Spectral Features in Magnetic Pulsation Events

Event	Maximum Point	UT	Frequency mHz	Period s	Power Density (nT) <sup>2</sup> /Hz	Bandwidth mHz	Max Power (nT) <sup>2</sup>	Equivalent rms Amplitude nT
5	83	2047:22	189	5.3	$1.48 \times 10^5$	~55	$8.1 \times 10^3$	90
	278	2054:37	108	9.3	$1.25 \times 10^6$	~55	$6.9 \times 10^4$	260
	241	2050:00	31	32	$1.01 \times 10^7$	15	$1.5 \times 10^5$	390
	105	2047:44	29	34	$3.88 \times 10^6$	23	$8.9 \times 10^4$	300
6	171	2032:50	70	14	$1.64 \times 10^6$	33	$5.4 \times 10^4$	230
	241	2034:00	46	24	$2.51 \times 10^7$	32	$8.0 \times 10^5$	900
9	350	2220:49	126	7.9	$1.25 \times 10^5$	~55	$6.9 \times 10^3$	80
	288	2219:47	61	16	$6.73 \times 10^5$	32	$2.2 \times 10^4$	150
	325	2220:24	61	16	$6.89 \times 10^5$	32	$2.2 \times 10^4$	150
	330	2220:29	20	50	$2.20 \times 10^6$	15	$3.3 \times 10^4$	180



**Figure 8.** Comparison between components in absorption and magnetic field during event 5. Coherence is shown between the two records (a) in the band 24 - 38.5 mHz (42 - 26 s), contrasted with the lack of coherence (b) in the band 84 - 115 mHz (11.9 - 8.7 s).

frequent occurrence suggests that they are real. The period 9.2 or 9.3 s occurs several times. From their weaker magnitude, lack of association between absorption and magnetic data (though they do occur in both), and occurrence away from the peak of the absorption event, it appears that fluctuations in the band 5.3 to 9.3 s (189 - 109 mHz) are different in nature from the slower variations.

## 7. Discussion and Conclusions

Generally speaking, the literature on pulsations in the Pi2 band discusses them in relation to substorm onset, to a localized current wedge connecting the current sheet in the magnetotail to the auroral *E* region, and to a westward traveling surge (WTS) in the luminous aurora preceding a major intensification and spreading

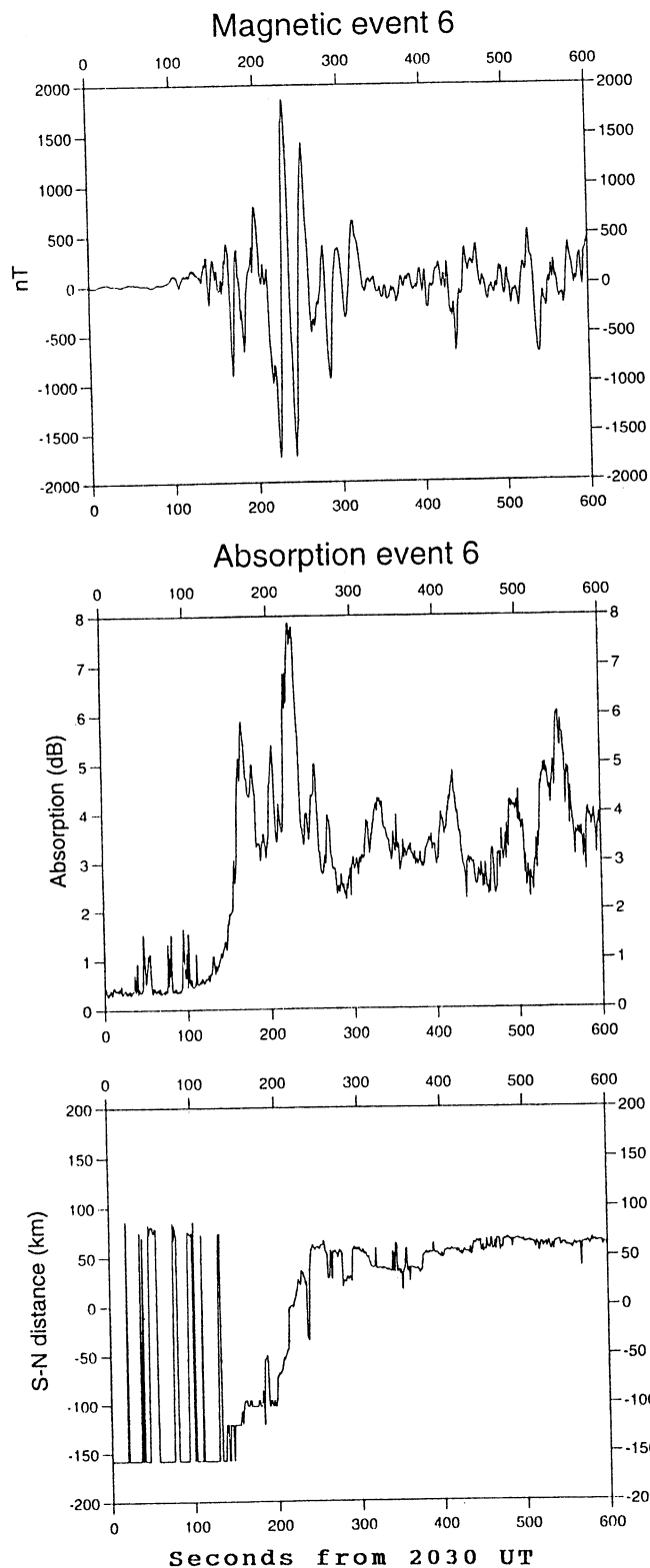


**Figure 9.** Event 6 (January 28, 1997, 2030 - 2100 UT).

(breakup) in the night sector. Some authors [e.g., Samson, 1982] have included auroral radio absorption in the picture, pointing out that the absorption spike seems to occur in the poleward edge of the surge. These are all related topics, relevant to the process(es) initiating the

nighttime aurora and associated phenomena, and are likely, therefore, to be of some fundamental importance to the topic.

There has been progress in knowledge of the spike event during recent years. As noted above, some of them indeed have the character of WTS, but in fact some absorption spikes move eastward and the more general characteristic is a poleward motion. It is also now known that the short duration of the spike is not because a narrow band of precipitation moves rapidly overhead, but because the spike itself is of short duration. The new feature reported here is that the spike contains temporal fine structure not dissimilar from magnetic Pi pulsations.

Reports of magnetic micropulsations related to substorm onset generally concern periods of 100 s or more, but the principal fine structure of absorption spikes is

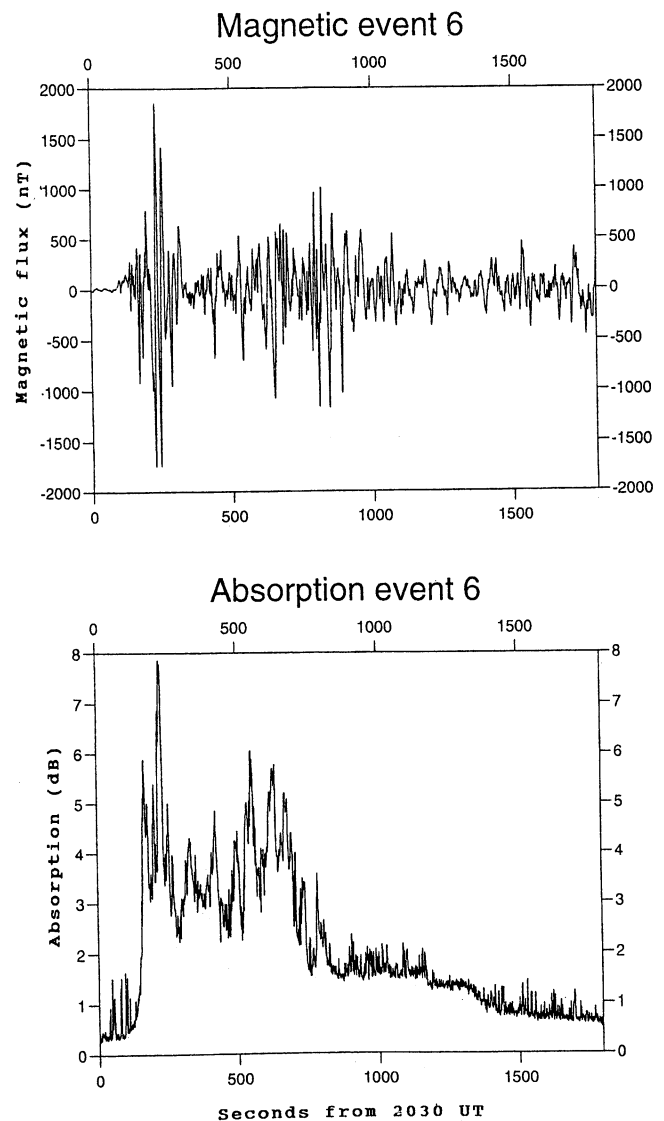


**Figure 10.** The first 600 s of event 6, showing details of the magnetic variations, the absorption, and the position of the absorption maximum from overhead in the N-S plane. Note the poleward motion during the first part of the absorption event.

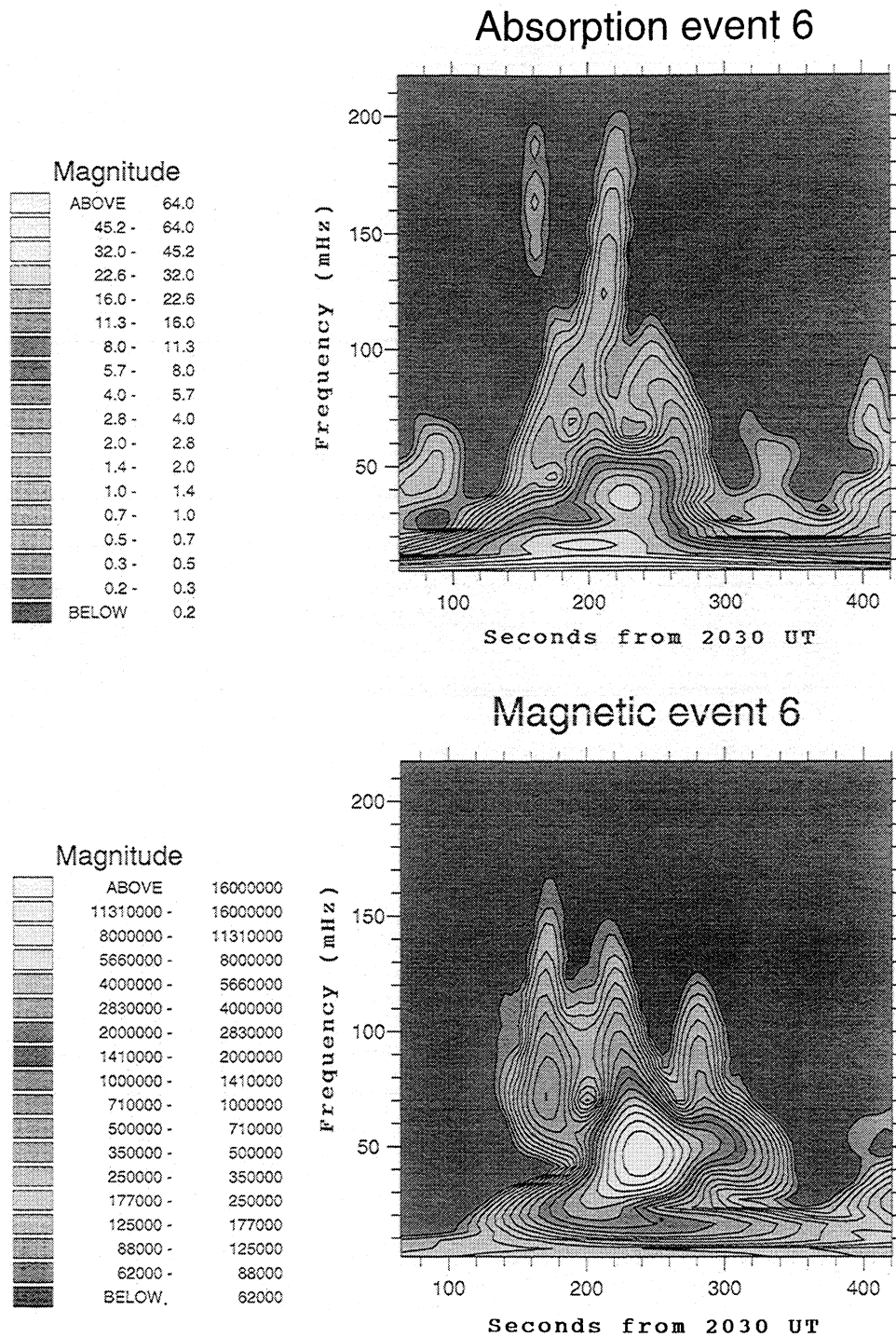


**Figure 11.** Magnetic and absorption spectra during the main part of event 6, both contoured on logarithmic scales. These spectra are not identical, but they have some marked points of similarity.

rather shorter than that, falling around the boundary between Pi1 and Pi2 in the usual classification. A periodicity of 100 s would not be apparent in a spike event because the typical event only lasts for 2 min; however, it is noted that the magnetic pulsations do not show long periodicities in the present examples either (see Figure 7 and 10).

Observations in space, however, reveal magnetic and electric pulsations over a wide band of frequencies, and

harmonics are commonly observed. *Takahashi et al.* [1984] reported spectra over about 8 to 70 mHz (including harmonics), a range of frequency similar to that found in the present study, though theirs were observed in the sunward part of the magnetosphere and thought to be generated by the action of the solar wind. *Holter et al.* [1996] used the Morlet wavelet to analyze an event observed at synchronous orbit at the onset of a substorm. They identified a short burst of pulsation at

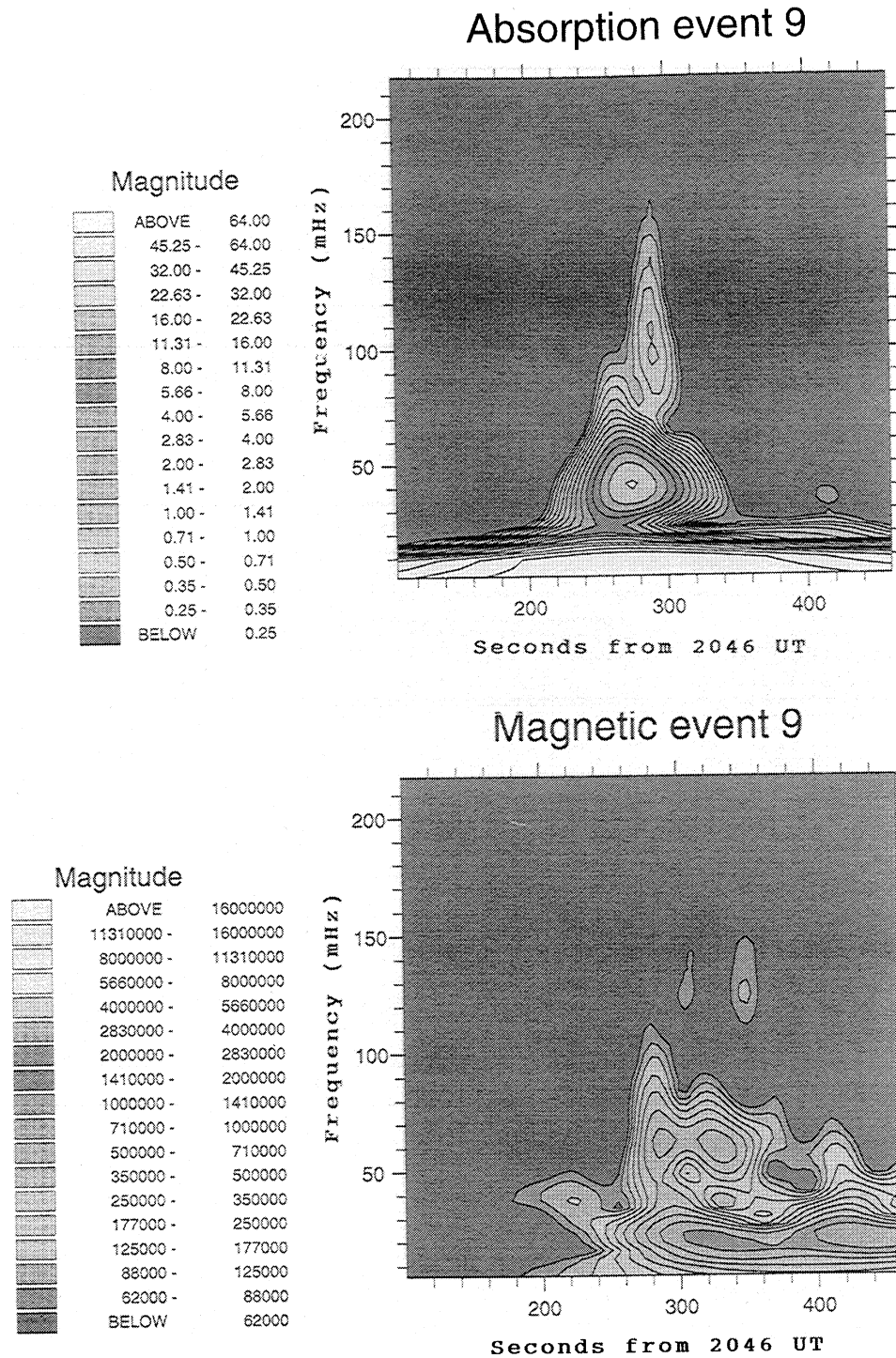


**Figure 12.** Magnetic and absorption spectra during event 9. This absorption spectrum is typical of spike events. The magnetic spectrum is the more complex of the two. In this example the principal absorption periodicity (41 mHz; 24 s) is the harmonic of the principal magnetic periodicity (20 mHz; 50 s). The third harmonic (61 mHz; 16 s) also appears in the magnetic spectrum.

20 – 25 mHz (40 – 50 s period), and from its polarization characteristics concluded that it was the second harmonic of a fundamental at 10 mHz which continued for a longer duration. (The wavelet spectrum of this event is strikingly similar to some of those presented in the present paper.) They suggested that the wave was

in the slow magnetosonic-shear Alfvén mode, and was a standing wave in the thin current sheet that forms prior to substorm onset. A substantial increase in energetic electron flux (> 22 keV) occurred at the substorm onset.

While the WTS is due to electrons in the keV range of



energies, the absorption spike is due to enhanced electron density in the *D* region and is therefore due to more energetic electrons, certainly extending to several tens of keV. The present results therefore indicate a connection between magnetic waves in the Pi1 – 2 range and fluctuations in the keV electrons causing auroral radio absorption. It cannot be stated with any certainty which is the cause and which the effect, but the observations that the waves tend to continue after the end of the absorption spike and that the detailed connection between them is strongest at the beginning of the event indicate at least that the magnetic pulsation is not a direct consequence of the electron precipitation. If it were, the micropulsation would fade with the absorption.

Observations of Pi2 in space show magnitudes of a fraction of a nanotesla to about 3 nT at geosynchronous orbit [McPherron, 1981], thus about 2% of the steady geomagnetic field strength at most. A similar fraction is observed at the ground in the present cases (i.e., 1000 nT in a total field of 50,000 nT). It is difficult to see how a magnetic variation of this small magnitude could modulate the flux of precipitating electrons by 20%. It seems more likely, then, that both sorts of pulsation are due to some third agent or process, presumably in the magnetosphere and probably related to the acceleration process at substorm commencement. The observation by Holter *et al.* [1996], referred to above, supports this view. On present evidence, the thin current sheet at substorm onset appears to be the most likely source.

We summarize the results as follows:

1. The spike event in auroral radio absorption, which frequently occurs at the beginning of a substorm, is subject to significant modulation at periodicities between 15 and 60 s (67 – 16 mHz). These have been studied using a wavelet technique.
2. The modulation appears to occur only in those spikes having poleward motion. The examples where the spike moved equatorward did not show a spectral maximum.
3. It appears that the same or related periodicities also occur in Pi pulsations observed simultaneously at the same location. The connection is only close during the initial period of the event while the spike event is moving poleward.
4. The results suggest that the electron precipitation at energies of tens of keV and the magnetic field are both modulated by a common source closely related to the mechanism of substorm onset, and likely to be in the thin current sheet of the magnetotail.
5. Both the absorption and the magnetic data also show weaker and more rapid pulsations in the band 5 – 10 s (200 – 100 mHz), which may occur at any time during the event, not only over the maximum. There is no evidence that these are closely related to each other, or to the slower modulation.

*Acknowledgment.* Michel Blanc thanks Martin Jarvis and Gunther Drevin for their assistance in evaluating this paper.

## References

- Coroniti F.V., R.L. McPherron, and G.K. Parks, Studies of the magnetospheric substorm, 3, Concept of the magnetospheric substorm and its relation to electron precipitation and micropulsations, *J. Geophys. Res.*, **73**, 1715, 1968.
- Detrick D.L., and T.J. Rosenberg, A phased-array radiowave imager for studies of cosmic noise absorption, *Radio Sci.*, **25**, 325, 1990.
- Hargreaves J.K., S. Browne, H. Ranta, A. Ranta, T.J. Rosenberg, and D.L. Detrick, A study of substorm-associated nightside spike events in auroral absorption using imaging riometers at South Pole and Kilpisjärvi, *J. Atmos. Terr. Phys.*, **59**, 853, 1997.
- Holter O., S. Perraut, A. Roux, C. Altman, A. Korth, H.L. Pecseli, J. Trulsén, and A. Pedersen, Structure of low frequency oscillations at substorm breakup, in Proceedings, Third International Conference on Substorms, Versailles, France, *Eur. Space Agency Spec. Publ.*, **ESA SP-389**, 393, 1996.
- Jacobs J.A., *Geomagnetic Micropulsations*, Springer-Verlag, New York, 1970.
- Liou K., C.-I. Meng, P.T. Newell, K. Takahashi, S.-I. Ohtani, A.T.Y. Lui, M. Brittnacher, and G.Parks, Evaluation of low-latitude Pi2 pulsations as indicators of substorm onset using Polar ultraviolet imagery, *J. Geophys. Res.*, **105**, 2495, 2000.
- McPherron R.L., Substorm associated micropulsations at synchronous orbit, *VLF Pulsations in the Magnetosphere*, (Ed. D.J. Southwood), Center of Academic Publications, Japan, Tokyo, 1981.
- Morlet J., G. Arens, I. Fourgeau, and D. Giard, Wave propagation and sampling theory, *Geophysics*, **47**, 203, 1982.
- Pashin A.B., K.-H. Glassmeier, W. Baumjohann, O.M. Raspopov, H.J. Opgenoorth, and R.J. Pellinen, Pi2 magnetic pulsations, auroral breakup, and the substorm current wedge: A case study, *J. Geophysics*, **51**, 223, 1982.
- Ranta H., A. Ranta, and J.K. Hargreaves, Small-scale structure of ionospheric absorption of cosmic noise during pre-onset and sharp onset phases of an auroral absorption substorm, *Geophysica*, **35**, 45, 1999.
- Samson J.C., Pi2 pulsations: High latitude results, *Planet. Space Sci.*, **30**, 1239, 1982.
- Samson J.C., and G. Rostoker, Polarization characteristics of Pi2 pulsations and implications for their source mechanism: Influence of the westward travelling surge, *Planet. Space Sci.*, **30**, 435, 1983.
- Takahashi K., R.L. McPherron, and W.J. Hughes, Multi-spacecraft observations of the harmonic structure of Pc 3-4 magnetic pulsations, *J. Geophys. Res.*, **89**, 6758, 1984.
- Torrence C., and G.P. Compo, A practical guide to wavelet analysis, *Bull. Am. Meteorol. Soc.*, **79**(1), 61, 1998.
- J.D. Annan and J.C. Hargreaves, Proudman Oceanographic Laboratory, Bidston Observatory, Prenton, Merseyside CH43 7RA, England.
- J.K. Hargreaves, Department of Communication Systems, University of Lancaster, Bailrigg, Lancaster LA1 4YR, England. (j.hargreaves@lancaster.ac.)
- A.Ranta, Sodankylä Geophysical Observatory, Tähteläntie 62, FIN-99600 Sodankylä, Finland. (aarne.ranta@sgo.fi)
- (Received September 9, 2000; revised December 6, 2000; accepted December 10, 2000.)